Applied Radiation and Isotopes 137 (2018) 219–224

Contents lists available at ScienceDirect

Applied Radiation and Isotopes

journal homepage: www.elsevier.com/locate/apradiso

Analysis on the emission and potential application of Cherenkov radiation in boron neutron capture therapy: A Monte Carlo simulation study

Di-Yun Shu[a], Chang-Ran Geng[a], Xiao-Bin Tang[a,b,*], Chun-Hui Gong[a], Wen-Cheng Shao[a], Yao Ai[a]

[a] Nanjing University of Aeronautics and Astronautics, Department of Nuclear Science and Engineering, 29 Yudao St., Nanjing 210016, China
[b] Collaborative Innovation Center of Radiation Medicine of Jiangsu Higher Education Institutions, 29 Yudao St., Nanjing 210016, China

HIGHLIGHTS

- Emission of Cherenkov photons in boron neutron capture therapy (BNCT) was explored.
- Cherenkov photons are generated from secondary charged particles of gamma in BNCT.
- Linear relation between boron concentration and Cherenkov photons was investigated.
- It presented the fundamental basis for applications of Cherenkov radiation in BNCT.

ARTICLE INFO

Keywords:
Cherenkov radiation
Boron neutron capture therapy
Boron concentration
Geant4

ABSTRACT

This paper was aimed to explore the physics of Cherenkov radiation and its potential application in boron neutron capture therapy (BNCT). The Monte Carlo toolkit Geant4 was used to simulate the interaction between the epithermal neutron beam and the phantom containing boron-10. Results showed that Cherenkov photons can only be generated from secondary charged particles of gamma rays in BNCT, in which the 2.223 MeV prompt gamma rays are the main contributor. The number of Cherenkov photons per unit mass generated in the measurement region decreases linearly with the increase of boron concentration in both water and tissue phantom. The work presented the fundamental basis for applications of Cherenkov radiation in BNCT.

1. Introduction

Boron neutron capture therapy (BNCT) is a binary targeted radiotherapy based on thermal neutron capture reaction with ^{10}B (Chadha et al., 1998; Miyatake et al., 2005). This treatment modality is possible to release a significant dose to neoplastic cells during a single fraction of neutron exposure, with producing little harm to surrounding normal cells (Coderre et al., 2003; Hopewell et al., 2011). The development of accelerator-based boron neutron capture therapy (AB-BNCT) have made this technique available for hospital (Kreiner et al., 2007, 2013; Elshahat et al., 2007; Ceballos and Esposito, 2009; Suzuki et al., 2009). However, there is still technology lacking for the boron concentration measurement, which is used for quality assurance and control of BNCT to ensure that the boron concentration meets the treatment requirement.

Cherenkov radiation is a kind of optical light emitted when a charged particle travels at a speed greater than the phase velocity of light in the medium (Cherenkov, 1934). More recently, Cherenkov radiation has been explored as a tool of quality assurance in conventional x-ray radiotherapy (Glaser et al., 2014; Helo et al., 2014a). Researchers have demonstrated that the Cherenkov emission imaging may able to be used for radiotherapy dosimetry (Glaser et al., 2015; Shu et al., 2016a). Moreover, Cherenkov radiation imaging for surface dose visualization during breast radiation therapy and rapid optimization of clinical treatment geometry in total skin electron beam therapy were explored (Jarvis et al., 2014; Andreozzi et al., 2016). Jang et al. analyzed the physics of Cherenkov radiation generation during proton therapy to explore the potential application (Jang et al., 2012; Helo et al., 2014b). However, there is no research on the underlining physics and characteristics of Cherenkov radiation in BNCT for potential applications, *e.g.* boron concentration measurement.

In this paper, the physics of Cherenkov radiation during BNCT was discussed, by means of simulations. Based on the water phantom, we investigated the relationship between boron concentration and the number of Cherenkov photons per unit mass under different conditions of measurement region. For the possible practical application, we analyzed the relationship between boron concentration and the number of Cherenkov photons per unit mass in biological tissue.

* Corresponding author at: Nanjing University of Aeronautics and Astronautics, Department of Nuclear Science and Engineering, 29 Yudao St., Nanjing 210016, China.
E-mail address: tangxiaobin@nuaa.edu.cn (X.-B. Tang).

https://doi.org/10.1016/j.apradiso.2018.04.012
Received 15 August 2017; Received in revised form 8 February 2018; Accepted 4 April 2018
Available online 06 April 2018
0969-8043/

Table 1
Cherenkov threshold energies of electron and proton in water and tissue.

Material	Cherenkov threshold energy (MeV)	
	Electron	Proton
Water (Refractive index = 1.33)	0.2635	483.87
Tissue (Refractive index = 1.41)	0.2134	391.83

2. Materials and methods

2.1. Generation of Cherenkov radiation in BNCT

According to the theory of Cherenkov radiation, only charged particle can directly generate Cherenkov radiation. Therefore, Cherenkov radiation cannot be generated from primary neutrons in BNCT; however, it can be originated from the secondary charged particles. Secondary charged particles in BNCT include recoil nuclei generated by neutron elastic and inelastic scatter process, secondary electrons generated by interactions between recoil nuclei and medium, secondary electrons and positrons generated by secondary gamma rays from neutron capture reaction. Most of the recoil nuclei are protons, whereas others are heavy ions. Threshold energies of generating Cherenkov radiation from electron and proton in different materials are shown in Table 1. The energies of recoil nuclei are far lower than the Cherenkov threshold energy attributing to the usage of neutron beam (< 1 MeV) in BNCT. Considering that the secondary electrons of recoil nuclei do not have sufficient energy to emit Cherenkov photons (Shu et al., 2016b), the contributors for emitting Cherenkov photons are secondary charged particles from gamma rays generated by neutron capture reaction during BNCT. The general generation process of Cherenkov photons during BNCT is shown in Fig. 1.

2.2. Monte Carlo simulation

Geant4 Monte Carlo toolkit in version 4.10.01.p01 was employed to simulate the particle-transportation process. The prepackaged QGSP_BIC_HP combined with optical physics list was invoked in Geant4 to perform a coupled simulation for neutrons, charged particles, photons, and Cherenkov photons (Agostinelli et al., 2003; Allison et al., 2006). The QGSP_BIC_HP package includes standard EM physics list, high-precision neutron model for neutrons below 20 MeV, quark gluon string model, binary cascade model, pre-computed and various de-excitation models. The neutron cross-section library in Geant4 comes from the ENDF/B-VII database. The generation and optical transport of Cherenkov photons depends on the optical physics list.

The geometric and beam setup in Geant4 are illustrated in Fig. 2. A

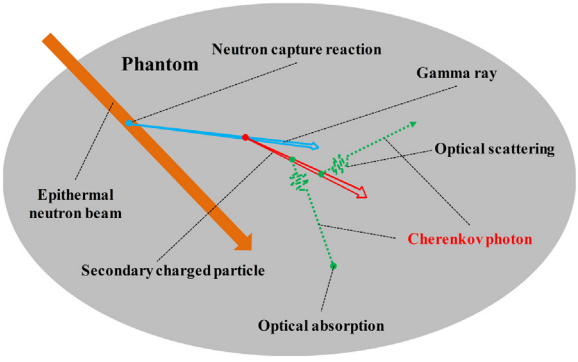

Fig. 1. Schematic of the generation of Cherenkov photons during BNCT. Different particles are plotted by different color, *i.e.* orange (neutron), blue (gamma), red (charged particle), green (Cherenkov photon) (For interpretation of the references to color in this figure legend, the reader is referred to the web version of this article.).

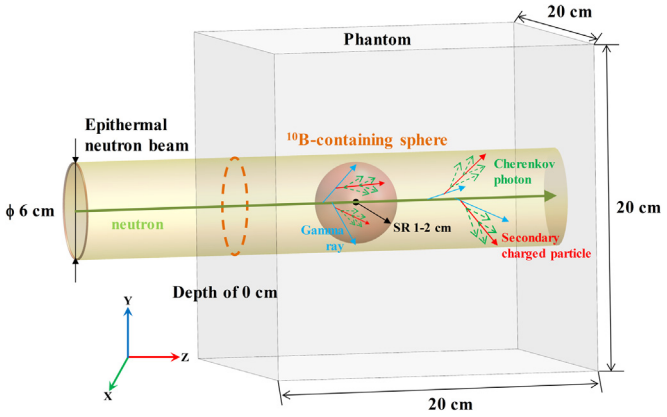

Fig. 2. Schematic of the geometry and beam setup in Geant4. The ^{10}B-containing sphere represents the measurement region. Lines of different colors present the generation process of Cherenkov photons.

20 cm × 20 cm × 20 cm water phantom was used in the simulation. A sphere containing ^{10}B was established in the center of the X-Y plane of the phantom. The ^{10}B-containing sphere was used to represent the measurement region. Measurement regions of different radii and depths were set to explore the relationship between boron concentration and Cherenkov photons under different conditions. It was set as a detector to score the quantities of interest. In this paper, the change rate of Cherenkov photons is defined as the variation of the number of Cherenkov photons per unit mass caused by the boron concentration change of 1 μg/g.

As a preliminary exploration, the setting of boron concentration distribution in the water phantom is an ideal situation. The boron concentrations in the sphere and the rest of the water phantom were assumed as 0–50 μg/g and 0 μg/g, respectively. To study the effect on biological tissues, the material of phantom replaced with soft tissue. The elemental composition of soft tissue is shown in Table 2. And the boron concentration distribution will be closer to the distribution in clinical trial case. The boron concentration of tumor/normal tissue ratio (T/N ratio) was set as 3.5. The boron concentrations in the sphere were assumed as 14–49 μg/g.

Epithermal neutron beam with a radius of 3 cm was employed to perpendicularly irradiate the phantom. The energy spectrum of the neutron beam was obtained from AB-BNCT, which is under construction by Neuboron Medtech Ltd. in China, as shown in Fig. 3 (Lee et al., 2014). All simulations were performed with 1.20×10^9 primary particles to keep the statistical uncertainty below 2% for the results in the measurement region.

3. Results and discussion

3.1. Water phantom

3.1.1. Dose and Cherenkov photons characteristics of epithermal neutron beam

The sphere with a radius of 1 cm was located at different depths to obtain the dose deposition by different particles and the generation of Cherenkov photons in the sphere. The boron concentration in ^{10}B-containing sphere was set as 30 μg/g to explore the characteristics of epithermal neutron beam. The results are shown in Fig. 4.

Boron dose and gamma dose reached the maximum values at depths

Table 2
Elemental composition of soft tissue.

Element	H	C	N	O	Na	P	S	Cl	K
Mass fraction (%)	10.5	25.6	2.7	60.2	0.1	0.2	0.3	0.2	0.2

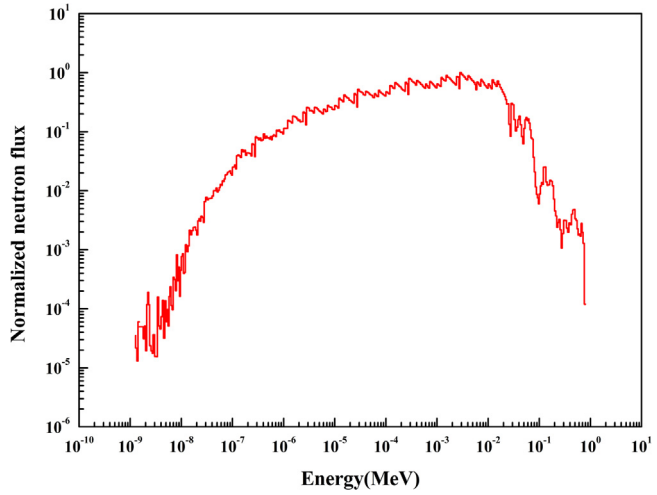

Fig. 3. Energy spectrum of neutron beam used in simulation (Lee et al., 2014). It was obtained from the source item of AB-BNCT in China.

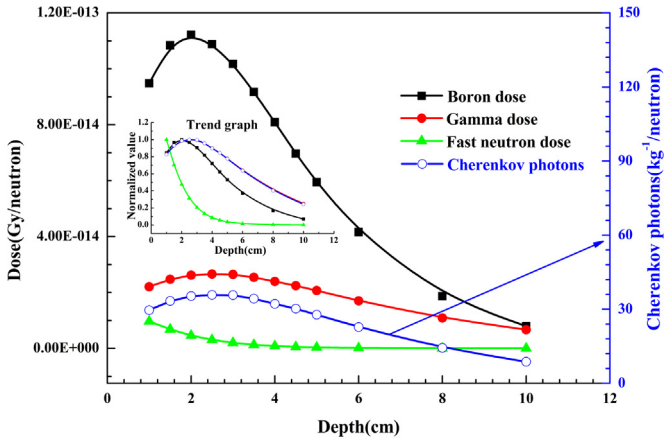

Fig. 4. Dose deposition and Cherenkov photons in the ^{10}B-containing sphere of different depths. Blue arrow represents that blue curve corresponds to the ordinate on the right. Normalization results are present in the scaled figure (For interpretation of the references to color in this figure legend, the reader is referred to the web version of this article.).

of 2.0 and 2.5 cm, respectively. The fast neutron dose rapidly decreases with the increase of depth. The depth distribution trend of Cherenkov photons was similar to the trend of gamma dose, which also reached the maximum value at the depth of 2.5 cm, as shown in the scaled panel in Fig. 4. This result showed that the generation of Cherenkov photons is closely related to gamma rays, indicating that using Cherenkov photons for gamma dose measurement may be one potential application in a neutron exposure situation.

3.1.2. Processes of Cherenkov photons generation in the ^{10}B-containing sphere

We further investigated the types of gamma rays and proportion of Cherenkov photons generated by secondary charged particles of gamma rays with different channels. The total number of Cherenkov photons generated by all particles was also recorded. In this simulation, ^{10}B-containing sphere with a radius of 1 cm was set at a depth of 2.5 cm.

The energy spectrum of gamma rays passing through the sphere is shown in Fig. 5. Gamma rays with energies of 0.478, 0.511, 0.871, 1.088, 2.184, 2.223 and 3.272 MeV were mainly observed. The 0.511 MeV gamma rays are from the process of positron annihilation. Cherenkov photon also can be generated by positron. In the following, secondary electrons of 0.511 MeV gamma rays and positrons are considered as the secondary charged particles of the corresponding high-energy gamma rays. Gamma rays with other energies are generated through neutron capture reaction with hydrogen and oxygen atoms.

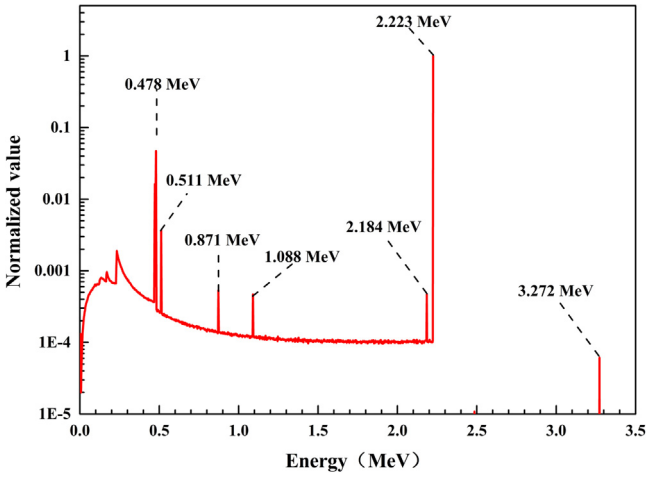

Fig. 5. Energy spectrum of gamma rays passing through the sphere. All the data is normalized by the value of 2.223 MeV gamma rays.

Fig. 6 depicts the number and proportion of Cherenkov photons generated by secondary charged particles of gamma rays with different energies. The total number of Cherenkov photons per unit mass and the number of Cherenkov photons per unit mass generated by secondary charged particles of gamma rays are equal, indicating that the interaction between secondary charged particles of gamma rays and the medium is the only way to emit Cherenkov photons during BNCT. The contribution of Cherenkov photons generated by secondary charged particles of gamma rays with energy of 2.223 MeV is about 99.893%, whereas the contributions of other gamma rays are very small. If the medium is a biological tissue, the types of gamma ray will be more than that of water. Considering the large atomic fraction (about 60%) and relatively high capture cross section (about 0.333 barns for thermal neutron) of hydrogen atom in human tissue, the secondary charged

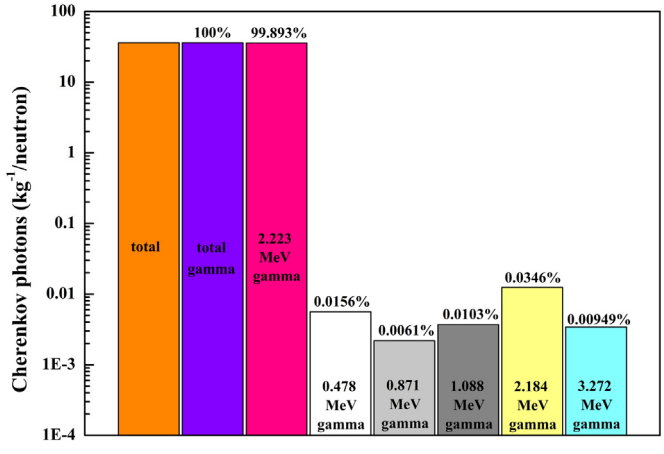

Fig. 6. Number and proportion of Cherenkov photons per unit mass generated by secondary charged particles of gamma rays with different energies.

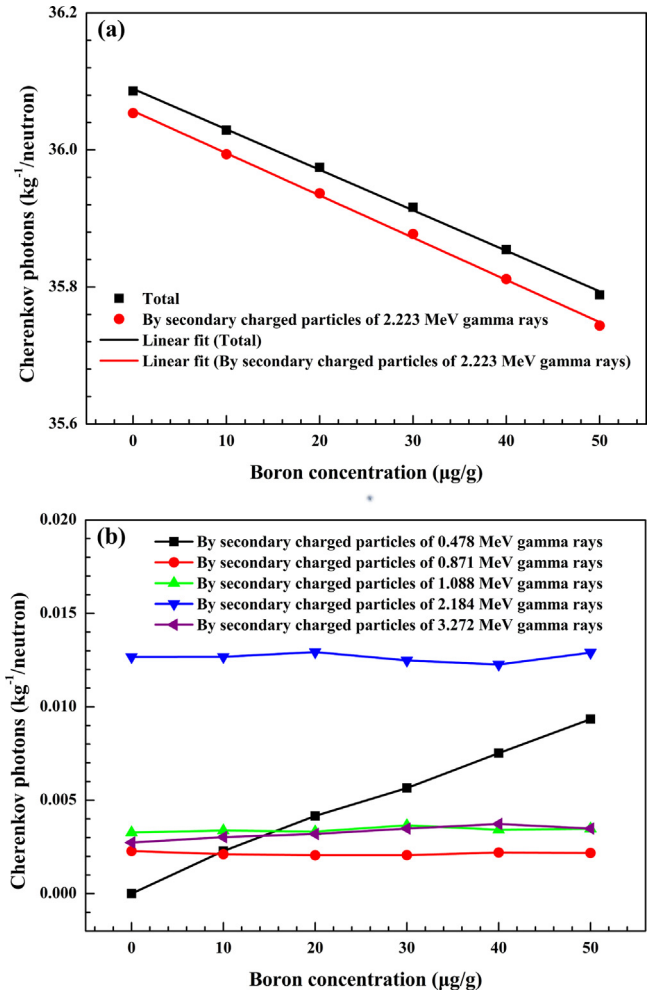

Fig. 7. Number of Cherenkov photons per unit mass generated by secondary charged particles of (a) gamma rays, 2.223 MeV gamma rays, and (b) gamma rays with other energies under different boron concentrations.

particles of gamma rays with energy of 2.223 MeV should also be the main contribution.

3.1.3. Variation of Cherenkov photons with boron concentration

To explore the potential application of Cherenkov photons in BNCT, the relationship between Cherenkov photons and boron concentration was investigated. The ^{10}B-containing sphere with a radius of 1 cm was set at a depth of 2.5 cm, and the number of Cherenkov photons per unit mass generated in the sphere was obtained when the boron concentration ranged from 0 μg/g to 50 μg/g. The number of Cherenkov photons per unit mass generated by secondary charged particles of gamma rays with different energies was also studied.

As shown in Fig. 7(a), the total number of Cherenkov photons per unit mass decreases linearly with the increase of boron concentration. The number of Cherenkov photons per unit mass generated by secondary charged particles of 2.223 MeV gamma rays shows the same trend. Fig. 7(b) shows that the number of Cherenkov photons per unit mass generated by secondary charged particles of 0.478 MeV gamma rays increases linearly with boron concentration, whereas the number of Cherenkov photons per unit mass generated by secondary charged particles of gamma rays with other energies is almost constant. The change rates of Cherenkov photons generated by secondary charged

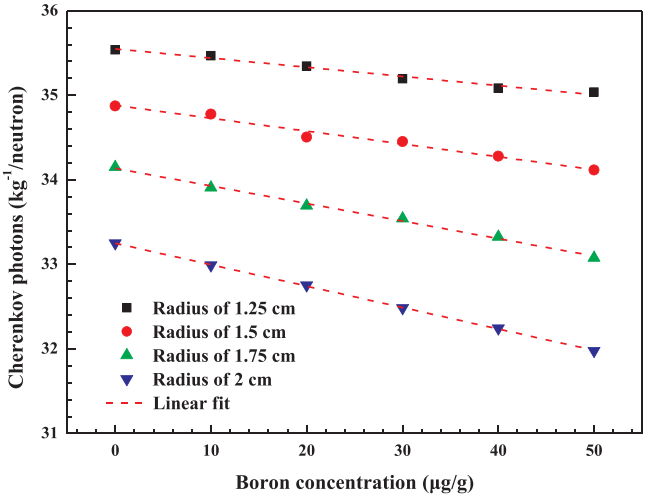

Fig. 8. Changes of Cherenkov photons with boron concentration under different radii of ^{10}B-containing sphere.

particles of all gamma rays, 2.223 MeV gamma rays and 0.478 MeV gamma rays are 0.006, 0.0062 and 0.0002 kg^{-1}/neutron/(μg/g), respectively. The changes of Cherenkov photons generated by secondary charged particles of 2.223 MeV gamma rays are much larger than the changes of Cherenkov photons generated by secondary charged particles of 0.478 MeV gamma rays. The overall changes of Cherenkov photons may have the potential to determine the boron concentration, although that the change rate of Cherenkov photons with boron concentration is relatively small. A high sensitivity optical detector may be required in practical application.

3.1.4. Relationship between boron concentration and Cherenkov photons under different radii of ^{10}B-containing sphere

The relationship between boron concentration and Cherenkov photons was explored with different sizes of ^{10}B-containing region. The ^{10}B-containing sphere with a radius from 1.25 cm to 2 cm was set at a depth of 2.5 cm. Fig. 8 shows the changes of Cherenkov photons with boron concentration under different radii of ^{10}B-containing sphere.

The linear relationship between boron concentration and Cherenkov photons also exists under different radii of the sphere. Under the same boron concentration, the number of Cherenkov photons per unit mass decreases with the increase of radius. This is because thermal neutron flux and spectrum are different at different depths, leading to the difference in the number of Cherenkov photons per unit mass. The change rate of Cherenkov photons with boron concentration is higher under the ^{10}B-containing sphere with bigger radius. This is due to that the ^{10}B-containing sphere with bigger radius will cause greater attenuation of the neutron flux when the change in boron concentration is the same.

3.1.5. Relationship between boron concentration and Cherenkov photons under different depths of ^{10}B-containing sphere

The depth of ^{10}B-containing sphere may influence the relationship between boron concentration and Cherenkov photons. The depth of ^{10}B-containing sphere with a radius of 1.5 cm was set from 1.5 cm to 3 cm. The changes of Cherenkov photons with boron concentration under different depths of ^{10}B-containing sphere are shown in Fig. 9.

As shown in Fig. 9, the number of Cherenkov photons per unit mass also decreases linearly with the increase of boron concentration. The number of Cherenkov photons per unit mass reaches the maximum

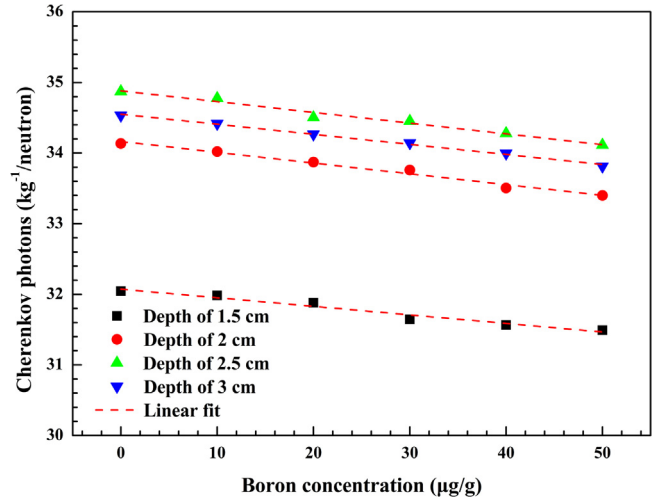

Fig. 9. Number of Cherenkov photons per unit mass with different boron concentrations under different depths of ^{10}B-containing sphere.

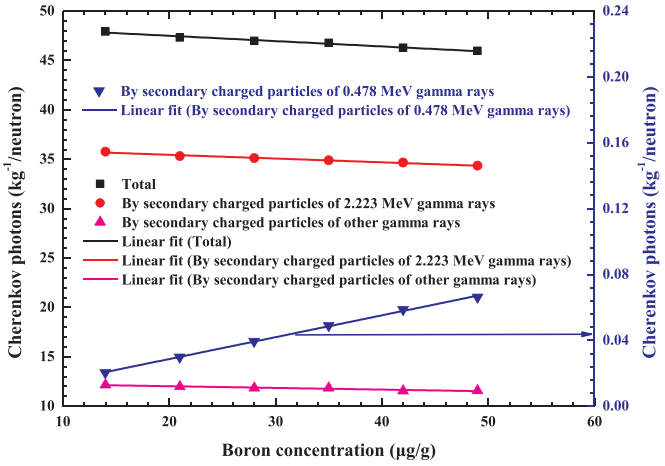

Fig. 10. Number of Cherenkov photons per unit mass generated by secondary charged particles of gamma rays with different energies under different boron concentrations. Blue arrow indicates that blue curve corresponds to the right y axis (For interpretation of the references to color in this figure legend, the reader is referred to the web version of this article.).

value at the depth of 2.5 cm, which is consistent with the results in Fig. 4. The minimum change rate is at the depth of 1.5 cm. The decreasing rate of the number of Cherenkov photons per unit mass with the increased boron concentration is similar for each depth.

3.2. Tissue phantom

We also studied the relationship between Cherenkov photons and boron concentration in tissue phantom, which has the same geometry setting with the water phantom. The ^{10}B-containing sphere with a radius of 1 cm was set at a depth of 2.5 cm. The boron concentrations in the sphere were ranged from 14 μg/g to 49 μg/g. Total number of Cherenkov photons per unit mass and the number of Cherenkov photons per unit mass generated by secondary charged particles of gamma rays with different energies in the sphere was obtained.

As shown in Fig. 10, the total number of Cherenkov photons per unit mass follows a linear relationship with boron concentration in tissue phantom. Due to the lower Cherenkov threshold energy in tissue, it will generate more Cherenkov photons comparing to that in water. The change rate of Cherenkov photons with boron concentration in tissue is larger than that in water, which is favorable for practical application. As the boron concentration increases, the number of Cherenkov photons per unit mass generated by secondary charged particles of 0.478 MeV gamma rays increases linearly because of the linear increase of boron atomic fraction. The number of Cherenkov photons per unit mass generated by secondary charged particles of 2.223 MeV gamma rays and other gamma rays decreases linearly with boron concentration. Table 3 shows the proportions of Cherenkov photons generated by secondary charged particles of gamma rays with different energies under different boron concentrations. The contribution of Cherenkov photons generated by secondary charged particles of 2.223 MeV gamma rays is about 74.6% in tissue phantom. The contribution of 0.478 MeV gamma rays is less than 0.2%, whereas the contribution of other gamma rays is about 25.3%.

4. Conclusions

Firstly, we discussed the physics of Cherenkov radiation during BNCT in a water phantom. Results showed that the only physics process to emit Cherenkov photons is through the interaction of secondary charged particles of gamma rays. Among all kinds of gamma rays, secondary charged particles of 2.223 MeV gamma rays are the largest contributors (99.893%) to the generation of Cerenkov photons in the water phantom. The linear relationship between boron concentration and the number of Cherenkov photons per unit mass has been investigated in the water phantom. Furthermore, when the radius or depth of ^{10}B-containing region is different, the linear relationship between boron concentration and Cherenkov photons also exists, except for the variations in change rate. We also found that the number of Cherenkov photons per unit mass also decreases linearly with boron concentration in tissue phantom, and it has a larger change rate than that in water phantom.

The linear relationship between Cherenkov photons and boron concentration can be determined when the size and position of measurement region and the condition of neutron source are certain. However, the sensitivity of boron concentration measurement based on Cherenkov radiation can be low, although the change rate of Cherenkov photons in tissue is larger than that in water. Given known situation, it is expected to be feasible for *in vitro* applications using Cherenkov radiation in BNCT with a highly sensitive optical detector and collection system. However, the *in vitro* measurement system of this method should be designed in the future, and the conversion relation between Cherenkov photons and boron concentration needs to be determined.

Table 3
Proportions of Cherenkov photons generated by secondary charged particles of gamma rays with different energies under different boron concentrations.

Boron concentration (μg/g)	14	21	28	35	42	49
Proportion (2.223 MeV gamma rays)	74.59%	74.64%	74.72%	74.58%	74.90%	74.68%
Proportion (0.478 MeV gamma rays)	0.04%	0.06%	0.08%	0.11%	0.13%	0.15%
Proportion (other gamma rays)	25.37%	25.30%	25.20%	25.31%	24.97%	25.17%

Furthermore, to experimentally test this method in BNCT is still challenging and will be further discussed.

For the *in vivo* application of boron concentration measurement, the linear relationship can be influenced by the neutron flux, neutron energy spectrum, and boron concentration condition of the surrounding regions. The diversity between different tissues is another important influencing factor. Considering the lower tissue penetration ability of Cherenkov photons, currently it is still very challenging to detect Cherenkov photons for *in vivo* application (Zhang et al., 2014). Nevertheless, many researchers are developing some technologies to improve the penetration of Cherenkov photon and imaging quality in the area of Cherenkov luminescence imaging (Wang et al., 2013). Even though, an application of the presented method in BNCT requires further research at this time, it still shows potential to be used for the determination of the ^{10}B concentation in BNCT.

Acknowledgments

This work was supported by the National Natural Science Foundation of China [Grant No. 11475087]; the National Key Research and Development Program [Grant No. 2017YFC0107700]; the National Key Research and Development Program [Grant No. 2016YFE0103600]; the Funding of Jiangsu Innovation Program for Graduate Education [Grant No. KYLX16_0351]; and the Priority Academic Program Development of Jiangsu Higher Education Institutions.

References

Agostinelli, S., Allison, J., Amako, K., et al., 2003. GEANT4—a simulation toolkit. Nucl. Instrum. Methods A 506, 250–303.
Allison, J., Amako, K., Apostolakis, J., et al., 2006. Geant4 developments and applications. IEEE Trans. Nucl. Sci. 53, 270–278.
Andreozzi, J.M., Zhang, R., Gladstone, D.J., Williams, B.B., Glaser, A.K., Pogue, B.W., Jarvis, L.A., 2016. Cherenkov imaging method for rapid optimization of clinical treatment geometry in total skin electron beam therapy. Med. Phys. 43, 993–1002.
Ceballos, C., Esposito, J., 2009. The BSA modeling for the accelerator-based BNCT facility at INFN LNL for treating shallow skin melanoma. Appl. Radiat. Isot. 67, S274–S277.
Chadha, M., Capala, J., Coderre, J.A., Elowitz, E.H., Iwai, J., Joel, D.D., Liu, H.B., Wielopolski, L., Chanana, A.D., 1998. Boron neutron-capture therapy (BNCT) for glioblastoma multiforme (GBM) using the epithermal neutron beam at the Brookhaven National Laboratory. Int. J. Radiat. Oncol. 40, 829–834.
Cherenkov, P.A., 1934. Visible emission of clean liquids by action of γ radiation. Dokl. Akad. Nauk SSSR 2, 451.
Coderre, J.A., Turcotte, J.C., Riley, K.J., Binns, P.J., Harling, O.K., Kiger, W.S., 2003. Boron neutron capture therapy: cellular targeting of high linear energy transfer radiation. Technol. Cancer Res. 2, 355–375.
Elshahat, B., Naqvi, A., Abdalla, K., 2007. Design calculations of an accelerator based BSA for BNCT of brain cancer. J. Radioanal. Nucl. Chem. 274, 539–544.
Glaser, A.K., Zhang, R., Gladstone, D.J., Pogue, B.W., 2014. Optical dosimetry of radiotherapy beams using Cherenkov radiation: the relationship between light emission and dose. Phys. Med. Biol. 59, 3789–3811.
Glaser, A.K., Andreozzi, J.M., Zhang, R., Pogue, B.W., Gladstone, D.J., 2015. Optical cone beam tomography of Cherenkov-mediated signals for fast 3D dosimetry of x-ray photon beams in water. Med. Phys. 42, 4127–4136.
Helo, Y., Rosenberg, I., D'Souza, D., MacDonald, L., Speller, R., Royle, G., Gibson, A., 2014a. Imaging Cherenkov emission as a quality assurance tool in electron radiotherapy. Phys. Med. Biol. 59, 1936–1978.
Helo, Y., Kacperek, A., Rosenberg, I., Royle, G., Gibson, A.P., 2014b. The physics of Cherenkov light production during proton therapy. Phys. Med. Biol. 59, 7107–7123.
Hopewell, J.W., Gorlia, T., Pellettieri, L., Giusti, V., H-Stenstam, B., Sköld, K., 2011. Boron neutron capture therapy for newly diagnosed glioblastoma multiforme: an assessment of clinical potential. Br. J. Radiol. 69, 1737–1740.
Jang, K.W., Yoo, W.J., Shin, S.H., Shin, D., Lee, B., 2012. Fiber-optic Cherenkov radiation sensor for proton therapy dosimetry. Opt. Express 20, 13907–13914.
Jarvis, L.A., Zhang, R., Gladstone, D.J., Jiang, S.D., Hitchcock, W., Friedman, O.D., Glaser, A.K., Jermyn, M., Pogue, B.W., 2014. Cherenkov video imaging allows for the first visualization of radiation therapy in real time. Int. J. Radiat. Oncol. 89, 615–622.
Kreiner, A.J., Kwan, J.W., Burlon, A.A., Paolo, H.D., Henestroza, E., Minsky, D.M., Valda, A.A., Debray, M.E., Somacal, H., 2007. A Tandem-electrostatic-quadrupole for accelerator-based BNCT. Nucl. Instrum. Methods B 261, 751–754.
Kreiner, A.J., Baldo, M., Bergueiro, J.R., et al., 2013. Accelerator-based BNCT. Appl. Radiat. Isot. 88, 185–189.
Lee, P.Y., Liu, Y.H., Jiang, S.H., 2014. Dosimetric performance evaluation regarding proton beam incident angles of a lithium-based AB-BNCT design. Radiat. Prot. Dosim. 161, 403–409.
Miyatake, S.I., Kawabata, S., Kajimoto, Y., et al., 2005. Modified boron neutron capture therapy for malignant gliomas performed using epithermal neutron and two boron compounds with different accumulation mechanisms: an efficacy study based on findings on neuroimages. J. Neurosurg. 103, 1000–1009.
Suzuki, M., Tanaka, H., Sakurai, Y., Kashino, G., Yong, L., Masunaga, S., Kinashi, Y., Mitsumoto, T., Yajima, S., Tsutsui, H., Sato, T., Maruhashi, A., Ono, K., 2009. Impact of accelerator-based boron neutron capture therapy (AB-BNCT) on the treatment of multiple liver tumors and malignant pleural mesothelioma. Radiother. Oncol. 92, 89–95.
Shu, D., Tang, X., Geng, C., Gong, C., Chen, D., 2016a. Determination of the relationship between dose deposition and Cherenkov photons in homogeneous and heterogeneous phantoms during radiotherapy using Monte Carlo method. J. Radioanal. Nucl. Chem. 308, 87–193.
Shu, D., Tang, X., Guan, F., Geng, C., Yu, H., Gong, C., Zhang, X., Chen, D., 2016b. Analysis of the relationship between neutron dose and Cherenkov photons under neutron irradiation through Monte Carlo method. Radiat. Meas. 3, 35–40.
Wang, Y., Liu, Y., Luehmann, H., Xia, X., Wan, D., Cutler, C., Xia, Y., 2013. Radioluminescent gold nanocages with controlled radioactivity for real-time in vivo imaging. Nano Lett. 13, 581–585.
Zhang, R., Andreozzi, J.M., Gladstone, D.J., Hitchcock, W.L., Glaser, A.K., Jiang, S., Pogue, B.W., Jarvis, L.A., 2014. Cherenkoscopy based patient positioning validation and movement tracking during post-lumpectomy whole breast radiation therapy. Phys. Med. Biol. 60, L1–L14.